Arabian Journal of Chemistry (2017) **10**, 194–205

King Saud University

Arabian Journal of Chemistry

www.ksu.edu.sa
www.sciencedirect.com

ORIGINAL ARTICLE

Preparation of nanostructured ruthenium doped titania for the photocatalytic degradation of 2-chlorophenol under visible light

Radwa A. Elsalamony *, **Sawsan A. Mahmoud**

Process Design and Development Department, Egyptian Petroleum Research Institute, Cairo, Egypt

Received 19 January 2012; accepted 17 June 2012
Available online 25 June 2012

KEYWORDS

Nanostructured Ru/TiO_2;
2-Chlorophenol;
Photocatalytic degradation;
Visible irradiation;
Chloride ions;
Acetate ions

Abstract Ru doped titania was prepared by the impregnation method and examined for the photocatalytic degradation of 2-chlorophenol at ambient conditions. Ru/TiO_2 photocatalysts with metal loadings of 0.2, 0.4, 0.6 and 0.8 wt% were prepared and characterized using TEM, XRD, FTIR, S_{BET} and EDX analyses. The degradation of 2-chlorophenol (2-CP) in the aqueous phase was investigated under irradiation at 254 nm, employing either photodegradation in the presence of titania, Ru doped titania or photolysis, to compare the efficiency of these photoinduced advanced oxidation techniques. Photocatalysis under visible irradiation was also investigated. The removal efficiency arrived at 50% using 0.2% Ru/TiO_2 catalyst.

1. Introduction

Chlorophenols such as 2-chlorophenol (2-CP), 4-chlorophenol (4-CP), 2,4-dichlorophenol (2,4-DCP) and pentachlorophenol (PCP) represent important water pollutants and have been named as priority pollutants by the USEPA (Callahan et al., 1979).

However; 2-chlorophenol is very hazardous in the case of skin contact (irritant), ingestion, inhalation and hazardous in the case of eye contact (irritant). Severe over-exposure can result in death. The stability of the C–Cl bond in halohydrocarbons is responsible for their toxicity and persistence in the biological environment (Roques, 1996). 2-Chlorophenol is very toxic and poorly biodegradable (Krijgsheld and van der Gen, 1986). A wastewater stream containing 2-CP over 200 mg l^{-1} may not be treated effectively by direct biological methods (Callahan et al., 1979). TiO_2 photocatalysis is currently accepted as one of the most promising technologies for the complete destruction and elimination of organic contaminants for environmental protection purposes (Shen et al., 2006; Sun et al., 2005; Fernandez et al., 2004). It is well known that the effectiveness of TiO_2 as a photocatalyst is very sensitive to its crystal phase, particle size, specific area, and pore structure. Among the advantages of titania over other

* Corresponding author. Address: 1 Ahmed Elzomor Street, Nasr City, Cairo, Egypt. Tel.: +20 02 24734983; mobile: +20 1144753475; fax: +20 22747847.
E-mail address: radwa2005@hotmail.com (R.A. Elsalamony).
Peer review under responsibility of King Saud University.

ELSEVIER Production and hosting by Elsevier

http://dx.doi.org/10.1016/j.arabjc.2012.06.008

photocatalysts, its excellent (photo) chemical stability, low cost and non-toxicity can be cited. However, its wide band-gap energy (ca. 3.0 e.v for rutile and 3.2 e.v for anatase) means that only 5% of the solar spectrum is used. Moreover, TiO_2 presents a relatively high electron–hole recombination rate which is detrimental to its photoactivity. In this sense, doping with metals or metal oxides could make a double effect:

(1) Firstly, it could reduce the band gap energy, thus shifting the absorption band to the visible region.
(2) Secondly, metals could provoke a decrease in electron–hole recombination rate, acting as electron traps.

There is considerable controversy on the effect of metal ions (Fox and Dulay, 1993). Several studies have reported that incorporation of transition metal ions can effectively enhance the efficiency of TiO_2-based catalytic systems (Tseng et al.,2002, 2004). Furthermore, the noble metal dopants can change the distribution of electrons because of their own catalytic properties and effectively prevent electron–hole recombinations, thereby enhancing the photocatalytic efficiency of TiO_2. However, there is considerable controversy on the effect of metal ions (Fox and Dulay, 1993; Day et al., 1990). Also, the loading level plays an important role as higher loading induces faster electron–hole recombination (Jaffrezic-Renault et al., 1986). Hence, it is of utmost importance to study the level of metal loading to exploit the maximum ability of noble metal-doped TiO_2 toward photoreduction.

Burns et al. (2002) investigated the photocatalytic degradation of 2-CP using sol–gel synthesized Nd-doped TiO_2 under UV irradiation. They reported that doping TiO_2 with Nd(III) reduced the photodegradation time due to the difference in the ionic radii of Nd(III) and Ti(IV). Much larger substitutional Nd caused localized charge perturbation and formation of oxygen vacancies which act as electron traps. Jung and coworkers (Jung, 2001; Jung et al., 2003) investigated the doping of transition metals such as Pd(II), Pt(IV), Nd(III), and Fe(III) in TiO_2 thin films synthesized by the metallorganic chemical vapor deposition method. They also demonstrated that Nd(III) doping improved the photodegradation of 2-CP under UV irradiation. Barakata et al. (2005) investigated the photocatalytic degradation of 2-CP using Co-doped TiO_2 nanoparticles under UV irradiation. Their study revealed that the photocatalytic activity strongly depends on Co doping concentration. The photodegradation process was optimized by using 10 mg l^{-1} Co-doped TiO_2 with a Co doping concentration of 0.036, after 3 h irradiation. They also established that the presence of Co ions in the TiO_2 structure caused a significant absorption shift toward the visible region. The photodegradation efficiency matched the maximum light absorption efficiency. Ru-doped visible light responsive TiO_2 was prepared to improve visible light absorption by Senthilnanthan et al. (2010). The photocatalytic activity of VLR Ru-doped TiO_2 was investigated to remove metsulfuron-methyl (MSM) in aqueous phase. The photocatalytic activity of VLR photocatalyst was significantly improved on the addition of Ru. The removal efficiency increased from 40% to 80%. The removal efficiency of MSM was proportional to the increasing Ru-doped TiO_2 under visible light. However, beyond the optimum concentration of 0.5 g l^{-1}, only a little improvement in the degradation of MSM was found.

In the present investigation, Ru doped mesoporous titania was prepared by the impregnation method with metal loadings of 0.2, 0.4, 0.6 and 0.8 wt% and characterized using TEM, XRD, FTIR, S_{BET} and EDX analyses. We carry out a series of investigations on the effect of Ru dopant level on TiO_2 mesoporous support, which in turn is directly related to its performance in the photocatalytic degradation of 2-CP. The study is also intended to give a picture of the influence of catalyst loading, dose of Ru, and phase transformation (anatase to rutile) on photocatalytic reduction of 2-chlorophenol. As doped TiO_2 is UV active (Nahar et al., 2006), we paid attention to improve activities in the visible range linking with Ru/doped catalysts.

2. Experimental

2.1. Preparation of the catalysts

For mesoporous TiO_2 materials (Huang et al., 2005), 3.6 g of tetrabutyl titanate was dissolved in absolute ethanol with a weight ratio of 1/7 under stirring. The resulting suspension was stirred for 3 h at room temperature, and then 5 ml of deionized water was added dropwise. The solution was stirred for an additional 2 h, followed by evaporation at 150 °C. The obtained solid product was exhaustively washed with deionized water and ethanol, dried at 80 °C overnight, and then calcined at 500 °C for 3 h.

Ru/TiO_2 samples with Ru loading ranging from 0.2% to 0.8% (w/w) using TiO_2 were prepared by the incipient wet impregnation method (Blackmond and Ko, 1984) with an aqueous solution of ruthenium trichloride trihydrate. An appropriate amount of the precursor, so as to obtain the desired Ru concentration in TiO_2, was mixed with TiO_2 in distilled water. The resulting slurry was subjected to continuous stirring at ambient temperature, and subsequently dried in an oven at 110 °C for 10 h. The solid residue was then crushed and calcined in air for 5 h.

2.2. Photolysis and photocatalysis experiments

500 cc of an aqueous solution containing 100 ppm of high purity 2-CP was subjected to UV irradiation using a 6 W lamp at a wavelength of 254 nm. All photodegradation experiments were conducted in a batch reactor at pH 6. The UV lamp was placed in a cooling silica jacket and placed in a jar containing polluted water. The catalyst was suspended in the solution with a magnetic stirrer at a controlled reaction temperature of 25 °C during the experimental period. At different irradiation time intervals, samples of the irradiated water were withdrawn for analysis using an HPLC chromatograph PerkinElmer (series 200) with photo-diode-array UV detector and a C18 column. The mobile phase was acetonitrile/water (60:40) injected in a rate of 1.0 ml min^{-1}.

The concentration of Cl^- and acetate ions produced in the solution during the photodegradation was determined by Ione Chromatography (IC Dionex-pac) attached with AS14 column of eluent consisted of 2:7 sodium carbonate/sodium bicarbonate mixture and the flow rate was 1.2 ml/min. In all cases, air was bubbled through the reaction mixture to ensure a constant dissolved O_2 concentration (3×10^{-4} mol dm^{-3}).

2.3. Physical characterization of the catalysts

N_2 physisorption was utilized to study the effect of the preparation and pretreatment process on the bulk Ru/TiO_2 samples. Characteristics such as BET surface area, pore size, and pore volume were examined. N_2 physisorption studies were carried out in a NOVA2000 gas sorption analyzer (Quantachrome Corporation) system. For each measurement, the sample was degassed at 250 °C for 3–4 h, and then analyzed at 77 K (liquid N_2 temperature). The surface areas and pore volumes were determined using the BET (Brunauer–Emmett–Teller) method from the adsorption branch in the relative pressure range of 0.05–0.35. The total pore volume of the samples was calculated from the nitrogen uptake at $P/P_o = 0.95$, using the BJH (Barrett–Joyner–Halenda) method from the isothermal desorption data.

XRD analysis was performed to determine the effects of Ru doping on the rutile and anatase concentrations. X-ray powder diffraction (XRD) patterns were obtained with a PANalytical X'Pert PRO diffractometer in reflection mode using CuKα radiation over the scan range of 2θ between 20 and 80 at 295 K, in order to identify the phase present.

FTIR were performed using ATI Mattson model Genesis Series (USA) Infrared spectrophotometer adopting KBr technique. For all samples, the KBr technique was carried out approximately in a quantitative manner since the weight of sample and that of KBr, were always kept constant.

The topography and particle size of Ru/TiO_2 were measured using JEOL transmission electron microscopy (TEM) operating at an accelerating voltage of 120 kV. The structure resolution of microscope is 0.2 nm. Prior to the analysis, the catalyst sample was ground into powder (using mortar and pestle) and then ultrasonically dispersed in a solvent and placed on a carbon-coated copper grid. The sample was allowed to dry before TEM analysis.

To confirm the presence of RuO_2 attained on TiO_2, EDX analysis was carried out. Energy Dispersive X-ray Spectroscopy (EDX or EDS) is a chemical microanalysis technique used in conjunction with SEM. EDX analysis was used to characterize the elemental composition of TiO_2.

3. Result and discussion

3.1. Characterization of Ru/TiO_2

The crystallinity of the prepared samples was examined by XRD analysis. XRD patterns of TiO_2-blank, and Ru doped (0.2, 0.4, 0.6 and 0.8 wt%) TiO_2 are shown in Fig. 1. TiO_2 is a mixture of anatase and rutile, The peaks at 2θ values of 25.3, 30.8, 37.8, 48.1, 53.9, 54.3, 56.6, 70.2 and 75.1, 82.7 were identified by comparison with literature data and confirm that the particles are polycrystalline with an anatase structure. Whereas; the peaks at 2θ values of 27.4, 36.1, 39.2, 41.3, 44.1, 62.8, 64.2, 69 were corresponding to rutile. The unsupported ruthenium oxide, which was produced from the decomposition of $RuCl_3{\cdot}xH_2O$, shows a pattern that matches the RuO_2 pattern in the JCPDS card indicating that after calcinations the Ru precursor decomposed to produce RuO_2. Therefore, RuO_2 should be observed in the unreduced Ru/TiO_2. As can be seen in Fig. 1, TiO_2 is a mixture of anatase and rutile, and most of the RuO_2 peaks are overlapped with rutile TiO_2. This makes it difficult to identify RuO_2 from the TiO_2 support with XRD. This RuO_2 behavior is also observed by Venkatachalam et al. (2007).

In Fig. 2, the percentages of rutile were calculated from X-ray diffraction intensities. The mass fraction of rutile, X_r, was determined by.

$$X_r = \frac{I_R}{0.8I_A + I_R} \tag{1}$$

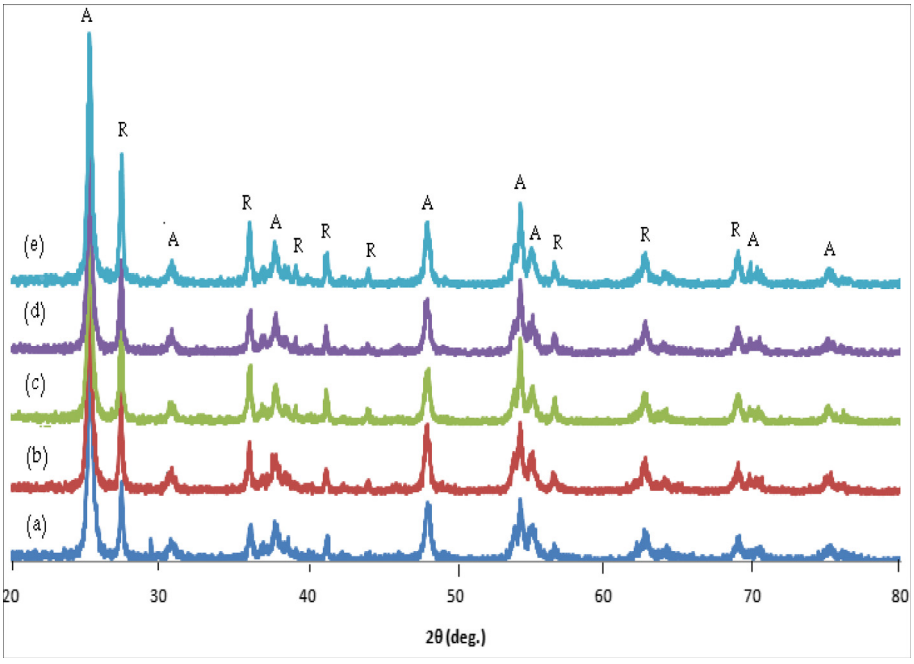

Figure 1 X- ray Diffraction spectra for (a) TiO_2, (b) 0.1 Ru/TiO_2, (c) 0.2 Ru/TiO_2, (d) 0.4 Ru/TiO_2, (e) 0.6 Ru/TiO_2, (f) 0.8 Ru/TiO_2.

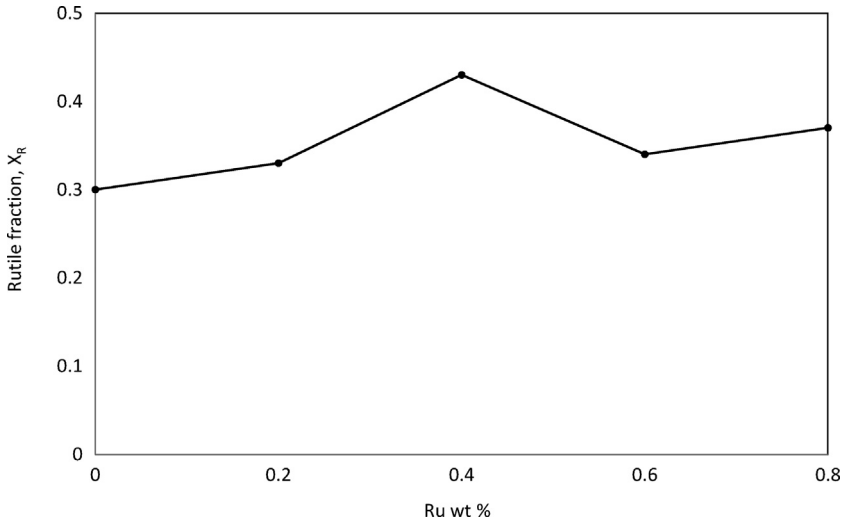

Figure 2 Rutile fraction of TiO_2 in Ru/TiO_2 catalysts as function of Ru ratio.

Table 1 Textural and structural properties of TiO_2 and Ru/TiO_2 samples.

Samples	Anatase/rutile[a]	Crystal size[a]		Specific surface area[b](cm^2/g)	Pore Radius Dv (r)[c](nm)	Total pore volume[c](cc/g)
		D_A	D_R			
TiO_2	70:30	33.5	50.6	27.8	6.2	0.123
0.2 Ru/TiO_2	66:33	23.7	27	28.5	6.6	0.125
0.4 Ru/TiO_2	57:43	28.8	50.6	23.4	7.9	0.107
0.6 Ru/TiO_2	66:34	19.4	23.7	24.7	6.6	0.12
0.8 Ru/TiO_2	63:37	33.6	67.5	22.9	6.1	0.094

[a] According to XRD analysis.
[b] BET surface area calculated from the linear portion of the BET plot in the relative pressure range of $p/p_0 = 0.05$–0.35.
[c] Pore radius and total pore volume estimated using BJH method from the isothermal desorption data.

where, I_R is the intensity of the predominant rutile peak (1 1 0) ($2\theta = 27.4°$), and I_A is the intensity of the predominant anatase peak (1 0 1) ($2\theta = 25.3°$) (Song et al., 2005). The effect of metal doped on TiO_2 phase transformation (anatase to rutile) is shown in Table 1. The Ru/TiO_2 samples showed a very similar isotherm to those of the TiO_2-blank (type IV). A representative adsorption–desorption hysteresis loop isotherm is shown in Fig. 3. The small figure inserted in Fig. 3 is the pore size distribution calculated from desorption data by the BJH method. The surface areas, average pore sizes, and pore radius of the analyzed samples are summarized in Table 1. According to Brunauer's classification samples are characterized by well-developed mesoporous structure (Tomul and Balci, 2009). The shape of the hysteresis loop is type H1closing at p/p_o ~0.6 according to the IUPAC classification that usually associated with pores consisting of agglomerates or compact of uniform spherical particles with regular arrays, whose pore size distribution are normally narrow and most of the pore diameters are in the range of 5–18 nm. (Leofanti et al., 1998). The least surface area of 22.9 m^2/g for Ru/Ti wt% 0.8, and the highest surface area of 28.5 cm^2/g were obtained when Ru/Ti wt% was 0.2. After the introduction of the Ru precursor and calcination to produce RuO_2 on the support, the surface area and total pore volume of the support were reduced; as metal loading increases from 0.4% to 0.8%; due to the presence of some RuO_2 in the pores.

Fig. 4 shows a summary of Raman spectra of Ru/TiO_2 catalysts. Structure of TiO_2 is confirmed in the FTIR spectrum. The peaks of TiO_2 anatase at ca. 527 cm^{-1} (Ti–O vibration), 633 cm^{-1}, and 450 cm^{-1} corresponding to the TiO_2 rutile crystalline phase were observed in all samples. The two bands appearing at 1564 and 1615 cm^{-1}, correspond to the stretching vibration of hydroxyl groups (O–H) and hydrogen-bonded surface water molecules (Brownson et al., 2005) in coordinated water, Ti–OH groups, or other hydrated species. Bands at 3383, 3427 cm^{-1}, are characteristic of, associated hydroxyl groups. Additional stronger bands at 3623, 3676 cm^{-1} are characteristic of tetrahedral coordinated vacancies, and designated Ti^{4+}-OH. Two strong absorbances at 3744 and 3825 cm^{-1} are due to octahedral vacancies and designated Ti^{3+}-OH (Madhu Kumar et al., 2000). Ru doped TiO_2 with different ratios of anatase to rutile, show that; the amount of surface adsorbed water and hydroxyl groups has little relation with crystallite phases (Liu et al., 2009).

The TEM images of undoped and Ru-doped TiO_2 are shown in Fig. 5. Blank TiO_2 and Ru-doped TiO_2 showed regular round shaped particles. There was no significant difference between the two particles. This was also previously confirmed from hysteresis loop of these samples. Small dark

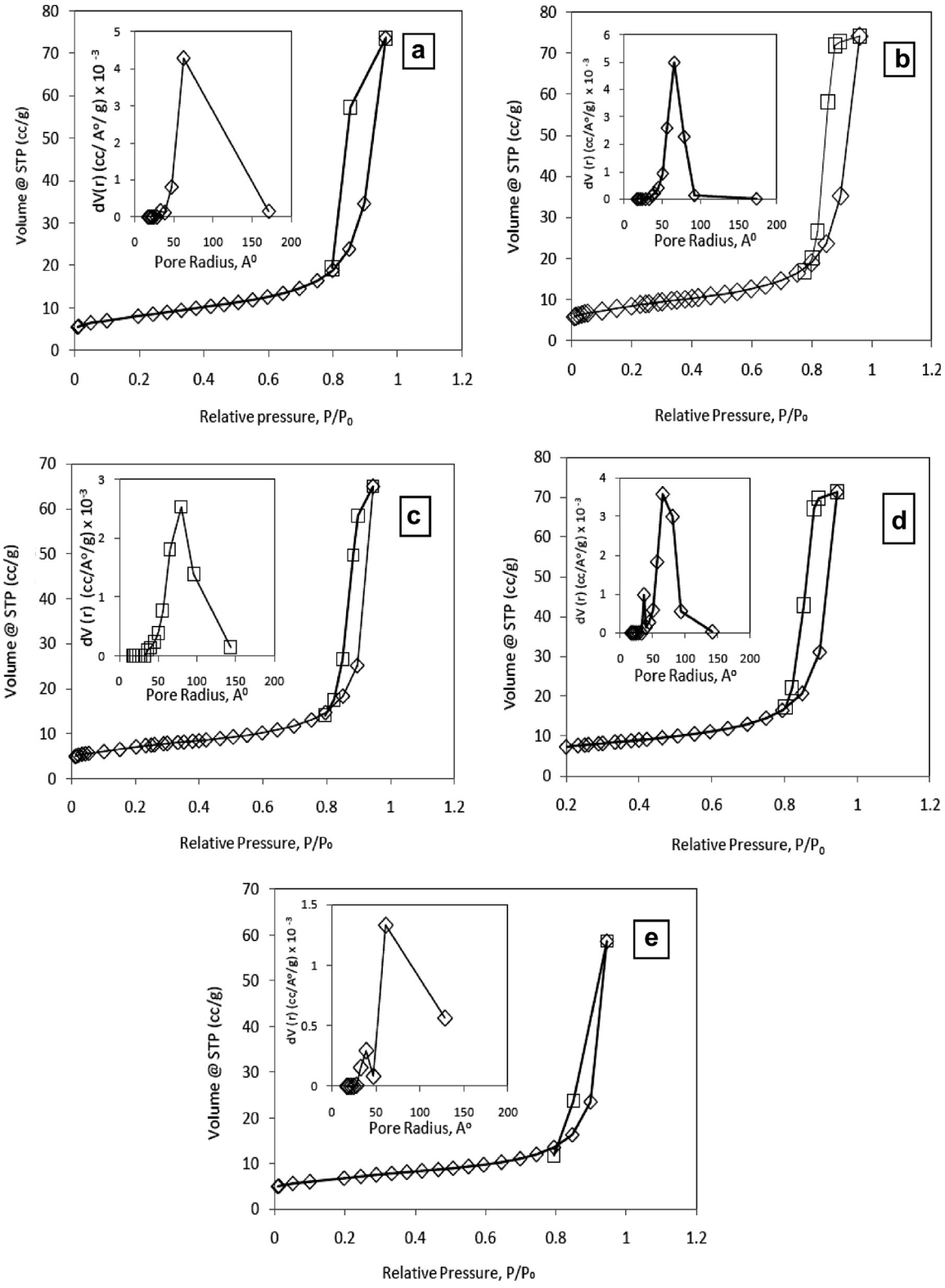

Figure 3 N_2 adsorption/desorption isotherms and pore size distribution plots of TiO_2(a), 0.2Ru/TiO_2(b), 0.4 Ru/TiO_2(c), 0.6 Ru/TiO_2(d), 0.8 Ru/TiO_2(e) samples.

spots seen are assumed as Ru particles and seem to be non-uniformly distributed among the TiO_2 particles with a particle size of approximately 14 nm. Furthermore; Shen et al. (2008) reported that Ru particles varied in width from 1 to 14 nm with the majority of the particles having width between 1

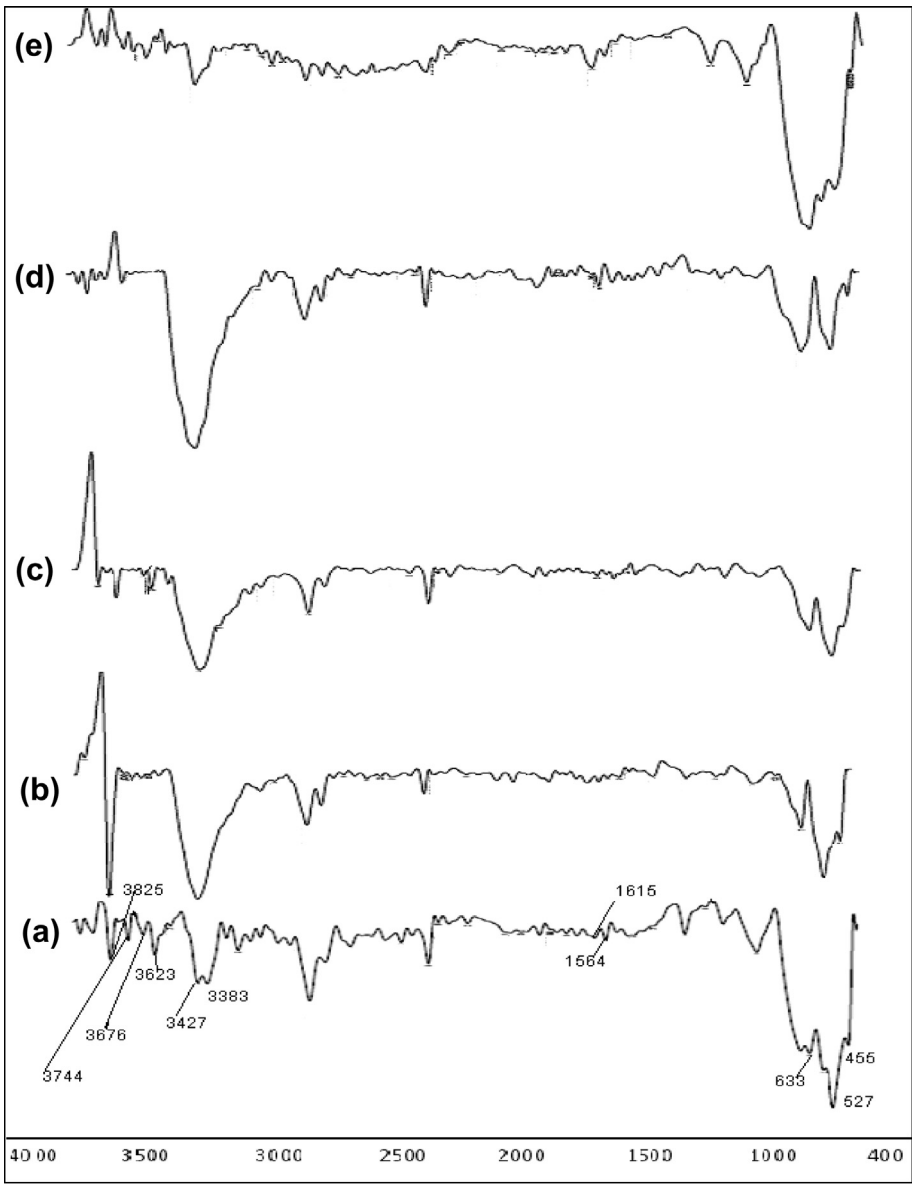

Figure 4 FTIR of (a) TiO_2, (b) 0.2Ru/TiO_2, (c) 0.4Ru/TiO_2, (d) 0.6Ru/TiO_2, (e) 0.8Ru/TiO_2 catalysts.

and 6 nm giving an average Ru particle size of 4.1 nm. This leads to spreading or covering by the layer of TiO_2.

A typical EDX pattern of the Ru/TiO_2 is shown in Fig. 6. The elemental composition of the samples was found to be 42.9% O, 56.9% Ti, 0.26% Ru for 0.2 Ru/TiO_2, and it was 56% O, 43.4% Ti, 0.45% Ru for 0.4 Ru/TiO_2 catalyst. However, it was confirmed in the presence of RuO_2 on TiO_2.

3.2. Direct photolysis

Photolysis of 2-CP by 254 nm reduced its concentration, up to 43% transformation after 60 min; as shown in Fig. 7. Previously, Ragaini et al. (2001) confirmed that 2-CP underwent reasonably fast photolysis under irradiation at 254 nm.

Fig. 8 shows the amount of chloride ions formed during the photodegradation process as a function of irradiation time. During photolysis; chloride ions reached 4 ppm after 60 min of irradiation time. This confirms that an efficient cleavage of the C–Cl bond occurs from the electronically excited state of 2-CP produced by direct light absorption at 254 nm. Furthermore, Barakata et al. (2005) reported the change in the pH is due to the liberation of HCl during the degradation reaction of 2-CP. The reaction can be represented mechanistically (Puma and Yue, 2002) and stoichiometrically (Rideh et al., 1997) as follows:

$$2\mathrm{CP}(\mathrm{C_6H_4OHCL}) \overset{hv,H2O}{\rightarrow} \mathit{Catechol}(\mathrm{C_6H_4(OH)_2})$$
$$\times \overset{hv}{\rightarrow} \mathrm{Intermediate} \overset{hv}{\rightarrow} 2\mathrm{HCl} + 12\mathrm{CO_2} + 4\mathrm{H_2O}$$

On the other hand, Fig. 9 shows the production of acetate ions under photolysis of 2CP. The higher acetate concentration at initial times decreases the pH value and encourages the

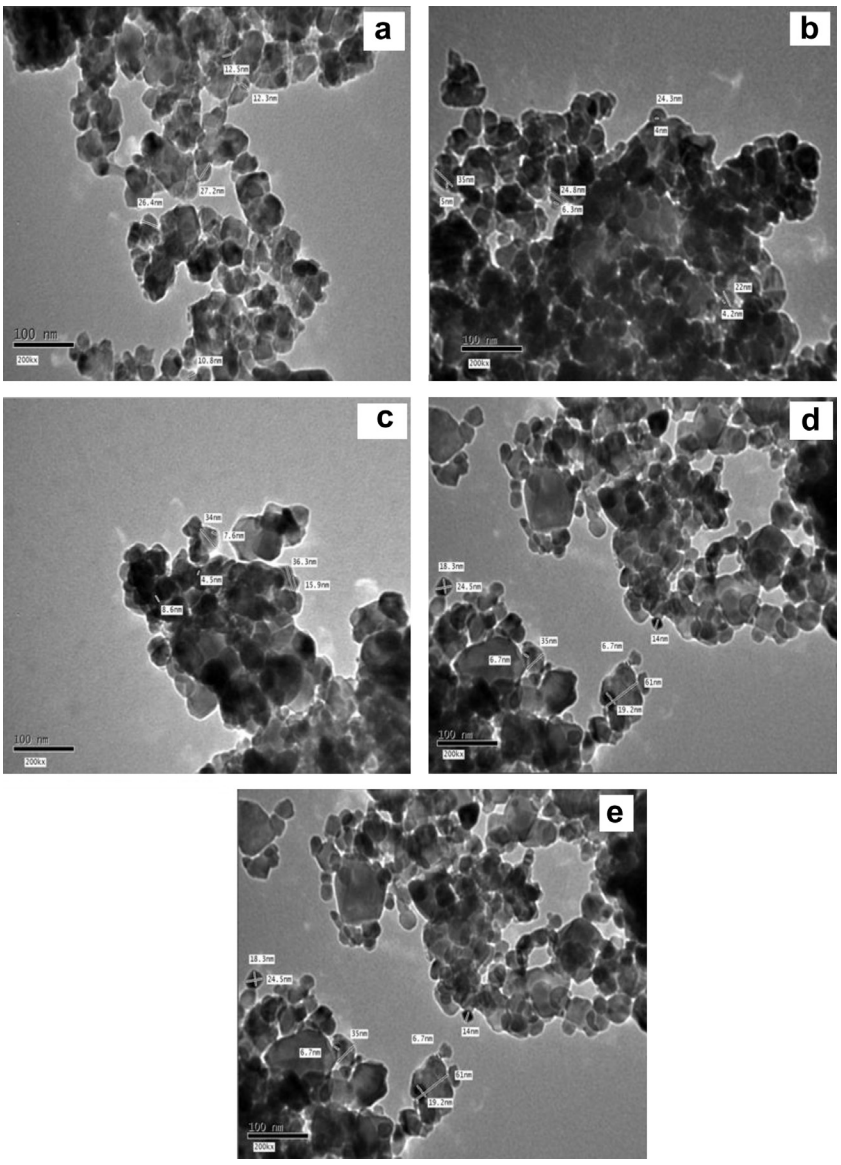

Figure 5 TEM micrograph of (a) TiO_2, (b) 0.2 Ru/TiO_2, (c) 0.4 Ru/TiO_2, (d) 0.6Ru/TiO_2, (e) 0.8 Ru/TiO_2.

formation of a positively charged TiO_2 ($TiOH_2^+$) surface which cannot provide hydroxyl groups needed for hydroxyl radical formation and consequently degradation rate is decreased (Barakata et al., 2005). This was also provided in our previous study on photocatalytic degradation of 2,4,6-trichlorophenol using Ti-MCM-41 catalysts (Aboul-Gheit et al., 2011). In general, the rapid degradation of formed acetate ions may be the rate determining step in the photolysis of 2CP.

3.3. Photocatalytic degradation in the presence of blank TiO_2

2-CP photocatalytic degradation was investigated under irradiation at 254 nm wavelength in the presence of mesoporous titania particles (UV + TiO_2). 2-CP photodegradation clearly proceeded faster in the absence of TiO_2 particles (Fig. 7). This may appear surprising at first sight. However, a similar behavior has been reported under irradiation either at 254 nm (Ilisz et al., 2002) or containing low wavelength components (Doong et al., 2001), while in general a rate increase was observed upon photocatalyst addition under irradiation at longer wavelengths (Ilisz et al., 2002). Of course, concomitant direct 2-CP photolysis and photocatalysis on TiO_2 occur under irradiation at 254 nm. The fact that, with increasing the fraction of light absorbed (and scattered) by the semiconductor particles, 2-CP underwent progressively slower degradation, indicates that the photocatalytic degradation path was slower than direct 2-CP photolysis. By contrast, photocatalytic conditions ensured faster mineralization. As shown in Fig. 7, a progressively higher percent mineralization was attained after 60 min irradiation in the presence of photocatalyst.

3.4. Effect of semiconductor content

In order to attain an optimum Ru dopant level, the target reaction was carried out on Ru doped TiO_2 with a dopant level of 0.2–0.8 wt% using UV light and the results are presented in Fig. 7. An interpretation of the reactivity order is difficult since it is probably the result of many factors: surface area,

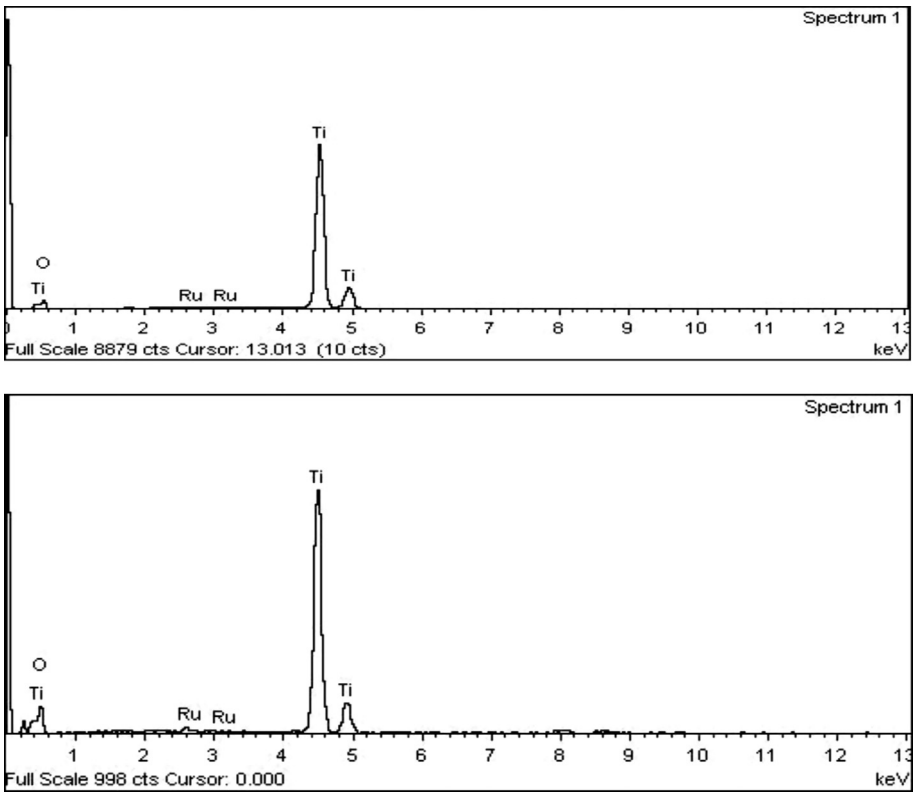

Figure 6 EDX spectrum of 0.2, 0.4 Ru/TiO_2 catalysts.

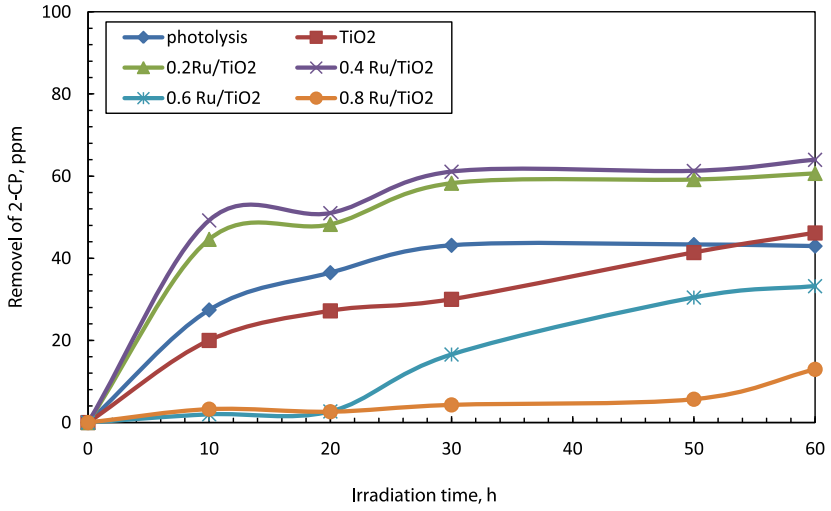

Figure 7 Effect of Ru doping concentrations on the 2-CP photodegradation using UV irradiation, catalyst loading 2 mg l^{-1}.

crystallinity, crystal size, etc. (Piera et al., 2003). An increase in the content of these metals leads to a decrease in the photocatalytic activity, while an increase in the anatase content in titanium dioxide leads to an increase in such activity (Kovalenko et al., 2003). The introduction of transition metals resulted in the change of the electronic environment of TiO_2. Based on the TEM results, Ru metals were adsorbed on the surface of TiO_2 as a little island of metal particles that act as the active sites of the photocatalytic reaction (Ozkan et al., 1998) and may favor separating charge carriers efficiently, inhibiting the recombination of electron–hole pairs, and ultimately causing enhancement of the reactivity. Barakata et al. (2005) suggested that by irradiation of the Co-doped TiO_2, Co(III) ions work as electron scavengers which may react with the superoxide species and prevent holes–electrons (h^+/e^-) recombination and consequently increase the efficiency of the photooxidation.

As shown in Fig. 7, the photodegradation efficiency of 2-CP increased with increasing Ru concentration, reaching a maximum value of 61% with sample containing 0.2 wt% Ru. A

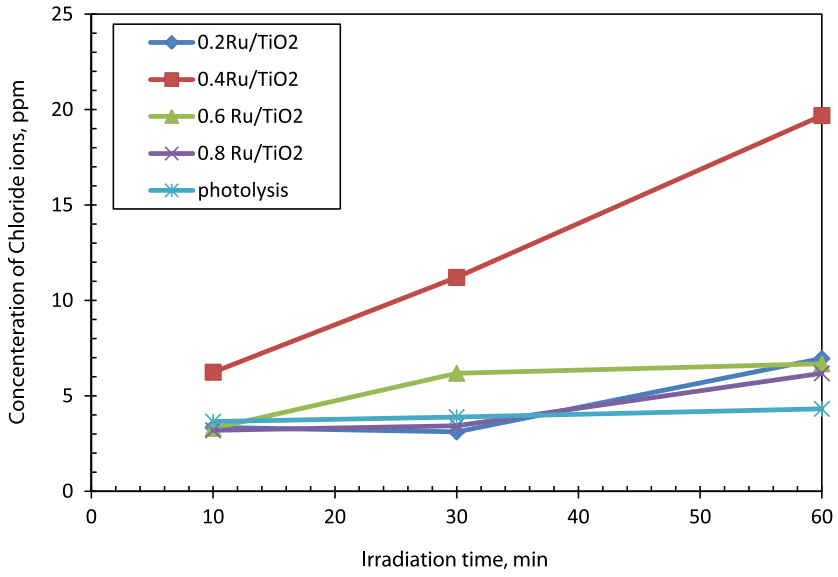

Figure 8 Formation of chloride ions during the photodegradation of 2-CP using UV light, catalyst loading 2 mg l^{-1}.

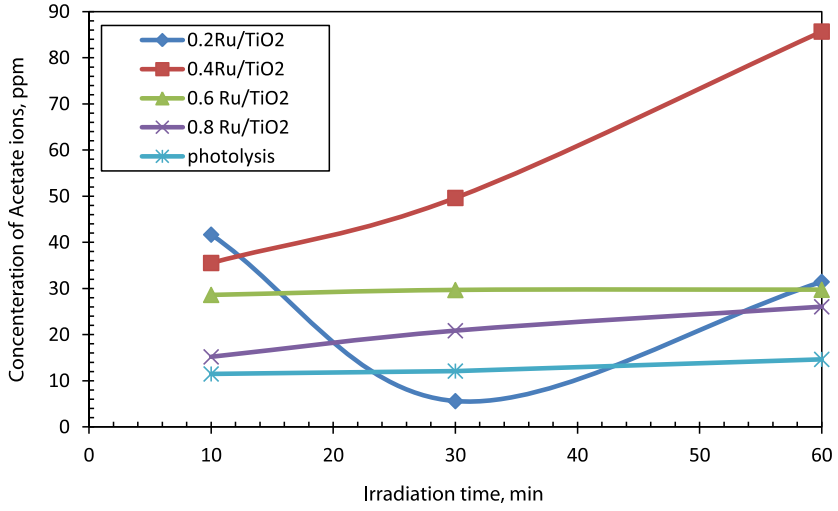

Figure 9 Formation of acetate ions during the photodegradation of 2-CP using UV light, catalyst loading 2 mg l^{-1}.

further increase in Ru concentration to 0.4 wt% resulted in a slight increase in the photodegradation efficiency to 63%.

On the contrary, if the Ru content is low in the case of 0.2 Ru/Ti wt%, there are fewer trapping sites available, thus reducing the activity. As a result; the activity of Ru/TiO_2 was dependent on the doping concentration and 0.4 wt% Ru/TiO_2 has turned out to be the optimum Ru doping level for photocatalytic reduction of 2-chlorophenol; because it has a high content of rutile as shown in Table 1. The enhanced light absorption activity of the mixed phases, suggested the transfer of photo generated electrons from a lower energy rutile to anatase electron site. This electron transfer would serve to reduce the recombination rate of anatase by increasing the separation between the electron and hole, resulting in greater catalytic reactivity (Bickley et al., 1991). Also, many catalytic "hot spots" may be located at the solid–solid interface of anatase and rutile, which is favorable for the improvement of photocatalytic activity (Li et al., 2007). However; Liu et al. (2009) studied the UV and visible-light photocatalytic activity of nitrogen doped TiO_2 with different ratios of anatase to rutile, and conclude that; nitrogen doped TiO_2 with a higher content of rutile can possess abundant surface water and hydroxyl groups, and a high photocatalysis efficiency. The highest chloride formation in the case of 0.4 Ru/TiO_2 catalyst (Fig. 8) indicates the rapid cleavage of C–Cl bond. However; a constant increase of acetate concentration (Fig. 9) provides this catalyst the ability to degrade aromatic rings during the photocatalytic process.

On the other hand; under irradiation at 254 nm, direct 2-CP photolysis appears to be faster than photocatalytic degradation using 0.6% and 0.8% Ru/TiO_2 catalysts. The reason attributed to the detrimental activity of Ru loading beyond 0.4 wt% is the increase in the recombination rate owing to the decrease in the distance between trapping sites in a particle

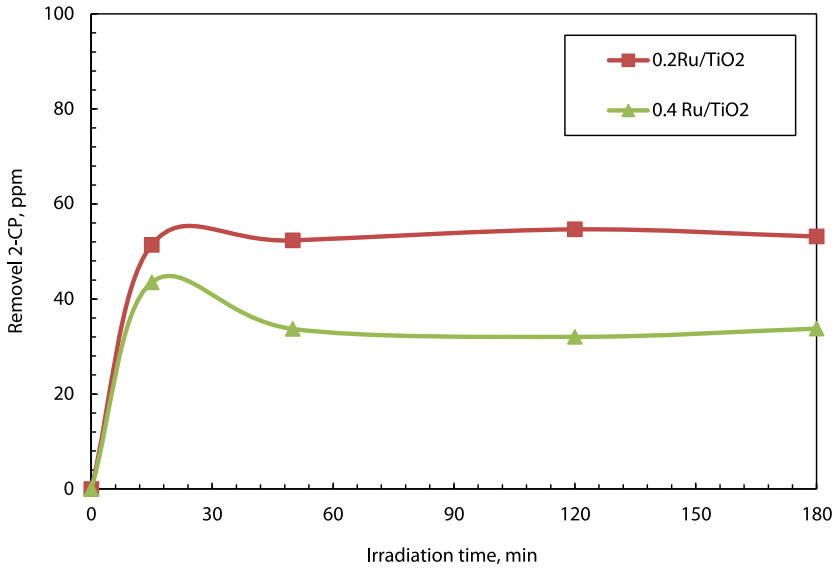

Figure 10 Effect of Ru doping concentrations on the 2-CP photodegradation under visible light, catalyst loading 4 mg l^{-1}.

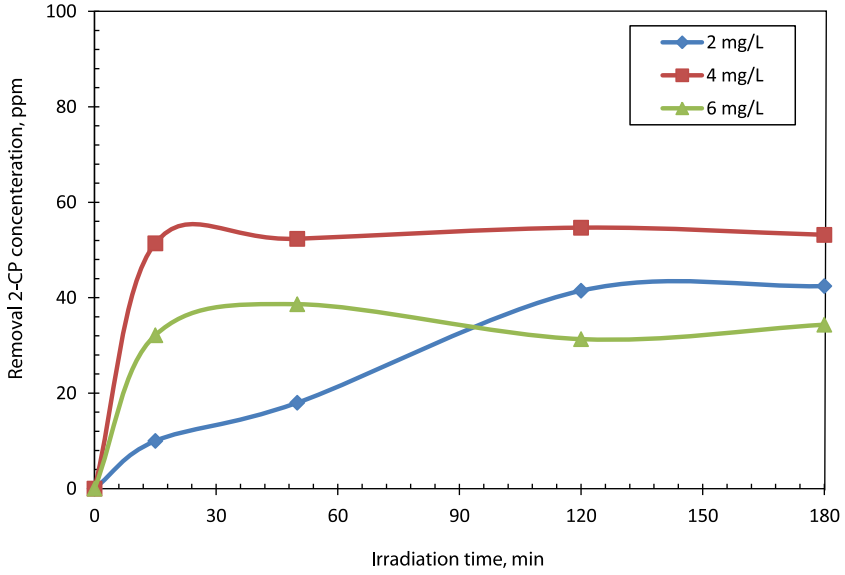

Figure 11 Effect of catalyst weight on photocatalytic degradation of 2-chlorophenol using visible light.

with a number of dopants (as shown in TEM images of 0.6, 0.8 Ru/TiO_2catalysts). Also; this result is approved by Nahar et al. (2009) whereas; 0.5% iron doped sample in the mixed phase catalyst decreased UV light absorption as compared to the undoped sample using the same preparation method, due to the recombination sites of Fe_2O_3. Iwasaki et al. (2000) and Choi et al. (1994) also confirmed the retarding effect of increasing Co(III) ion doping ranging from 0.004 to 0.14 on the photocatalytic activity of TiO_2 under UV light irradiation. Moreover, the results of BET surface area could suggest that some photocatalytic active sites of the TiO_2 surface are blocked by Ru particles due to decreasing pore volume as doped metal ratio increases beyond 0.4%, resulting in lower catalytic activity.

3.5. Photocatalytic degradation using visible light

Effect of Ru doping concentrations on the 2-CP photodegradation under visible light is shown in Fig. 10. The photodegradation efficiency of 2-CP reaches a maximum value of 53% with sample containing 0.2 wt% Ru. A further increase in Ru concentration to 0.4 wt% resulted in decrease in the photodegradation efficiency to 34%. Besides, anatase and rutile ratio, the crystal size of catalyst particles and surface area are also important factors for the photocatalytic activity. For 0.4% Ru/TiO_2 catalyst, the crystal size of rutile is increased (Table 1). Its surface area is decreased and the pore volume is decreased. Thus, the 0.2% Ru/TiO_2 with a higher anatase ratio structure, larger surface area large pore volume and smaller

crystal size has the best photocatalytic oxidation efficiency in the visible region. Pore volume is related to the diffusion of pollutants and samples during the photocatalytic reaction. The higher the pore volume of the samples, the diffusion between pollutants and samples becomes rapid and fast (Guo et al., 2009).

Based on the observation of Ku et al. (1996) study, the differences between the global photocatalytic destruction rates of 2-CP by various forms of TiO_2 particles might be attributed to the difference of the surface area of TiO_2, not to the difference of the crystal properties in this study.

In addition, the activity has a direct correlation with the amount of ·OH groups on the surface (Tsai and Cheng, 1997); as previously shown in FTIR spectrum, the 0.2 Ru/TiO_2 catalyst has a high amount of •OH groups on the surface than 0.4 Ru/TiO_2.

3.6. Effect of 0.2 Ru/TiO_2 loading

The photocatalytic degradation of 2-CP was carried out over a 0.2 Ru/TiO_2 catalyst at a different loading of 2–6 mg l^{-1} in order to optimize catalyst loading during the visible irradiation process. A significant increase in the degradation of 2-CP as catalyst loading increases from 2 mg l^{-1} to 4 mg l^{-1}; is illustrated in Fig. 11.

The decrease in the degradation of 2-CP above 4 mg l^{-1} may be attributed to the scattering effect of light caused by the high concentration of photocatalyst. The photodecomposition rates of pollutants are influenced by the active site and the photoabsorption of the catalyst used. Adequate loading of the catalyst increases the generation rate of electron/hole pairs for enhancing the degradation of pollutants. However, addition of a high dose of the semiconductor decreases light penetration by the photocatalyst suspension and reduces degradation rate (Doongr and Chang, 1998).

4. Conclusion

From the study of the above work, the following conclusions can be drawn:

- Enhancement of the photocatalytic activity of TiO_2 for photocatalytic degradation of 2-CP by doping Ru has been achieved.
- The mineralization of 2-CP is demonstrated by production of chloride and acetate ions.
- The entry of Ru into the lattice of TiO_2 is evidenced by XRD, SEM-EDX and TEM studies.
- 0.4 wt% Ru/TiO_2 has turned out to be the optimum Ru doping level for photocatalytic reduction of 2-chlorophenol using UV light; because it has a high content of rutile. The enhanced light absorption activity of the mixed phases, suggested the transfer of photo generated electrons from a lower energy rutile to anatase electron site. This electron transfer would serve to reduce the recombination rate of anatase by increasing the separation between the electron and hole, resulting in greater catalytic reactivity.
- On the other hand; the 2% Ru/TiO_2 with the optimum catalyst loading of 4 mg l^{-1}, provided photodegradation efficiency of 2-CP reaching a maximum value of 53% using visible light. The incorporation of Ru in TiO_2 led to large surface area and high pore volume values. This also led to the formation of more electron capture traps, which contribute to high separation efficiency of photogenerated carriers.

References

Aboul-Gheit, A.K., Abdel-Hamid, S.M., Mahmoud, S.A., El-Salamony, R.A., Valyon, J., Mihályi, M.R., Szegedi, Á., 2011. Mesoporous Ti-MCM-41 materials as photodegradation catalysts of 2,4,6-trichlorophenol in water. J. Mater. Sci. 46, 3319–3329.

Barakata, M.A., Schaeffera, H., Hayesa, G., Ismat-Shah, S., 2005. Photocatalytic degradation of 2-chlorophenol by Co-doped TiO_2 nanoparticles. Appl. Catal. B: Environ. 57, 23–30.

Bickley, R., Gonzalea-Carreno, T., Lees, J., 1991. A structural investigation of titanium dioxide photocatalysts. J. Solid State Chem. 92, 178–190.

Blackmond, D.G., Ko, E.I., 1984. Preparation and characterization of well-defined Ni/SiO_2 catalysts. Appl. Catal. 13, 49–68.

Brownson, J.R.S., Tejedor-Tejedor, M.I., Anderson, M.A., 2005. Photoreactive anatase consolidation characterized by FTIR spectroscopy. Chem. Mater. 17, 6304–6310.

Burns, A., Li, W., Baker, C., Shah, S.I., 2002. Sol–gel synthesis and characterization of neodymium-ion doped nanostructured titania thin film. Mater. Res. Soc. Symp. Proc. 703, 193–198.

Callahan, M.A., Slimak, M.W., Gabel, N.W., May, I.P., Foeler, C.F., Freed, J.R., Jennings, P., Durfee, R.L., Whitemore, F.C., Maestri, B., Mabey, N.R., Holt, B.R., Gould, C., 1979. Water-related Environmental Fate of 129 Priority Pollutants, No. 84-1-8, EPA-440/4-79-029b.. vol. 2 US Environmental Protection Agency, Washington, DC.

Choi, W., Termin, A., Hofmann, M.R., 1994. Effects of metal-ion dopants on the photocatalytic reactivity of quantum-sized TiO_2 particles. Angew. Chem., Int. Ed. Engl. 33, 1091–1092.

Day, V.W., Klemperer, W.G., Main, D.J., 1990. Niobotungstate, $Nb_2W_4O_{19}^{4-}$ and triphosphate, $P_3O_9^{3-}$, complexes of (cyclooctadiene)iridium(I): synthesis, structure, and stability of tetra-n-butylammonium salts of $\{[(C_8H_{12})Ir]_5(Nb_2W_4O_{19})^2\}^{3-}$,$\{[(C_8H_{12})Ir]_2H(Nb_2W_4O_{19})^2\}^{5-}$,and $[(C_8H_{12})Ir(P_3O_9)]^{2-}$. Inorg. Chem. 29, 2345–2355.

Doong, R.-A., Chen, C.-H., Maithreepala, R.A., Chang, S.-M., 2001. The influence of pH and cadmium sulfide on the photocatalytic degradation of 2-chlorophenol in titanium dioxide suspensions. Water Res. 35, 2873–2880.

Doongr, A., Chang, W.H., 1998. Photodegradation of parathion in aqueous titanium dioxide and zero valent iron solutions in the presence of hydrogen peroxide. J. Photochem. Photobiol. A: Chem. 116, 221–228.

Fernandez, J., Kiwi, J., Baeza, J., Freer, J., Lizama, C., Mansilla, H.D., 2004. Orange II photocatalysis on immobilised TiO_2: effect of the pH and H_2O_2. Appl. Catal. B: Environ. 48, 205–211.

Fox, M.A., Dulay, M.T., 1993. Heterogeneous photocatalysis. Chem. Rev. 93, 341–357.

Guo, B., Shen, H., Shu, K., Zeng, Y., Ning, W., 2009. The study of the relationship between pore structure and photocatalysis of mesoporous TiO_2. J. Chem. Sci. 121, 317–321.

Huang, D., Luo, G.S., Wang, Y.J., 2005. Using phosphoric acid as a catalyst to control the structures of mesoporous titanium dioxide materials. Micropor. Mesopor. Mater. 84, 27–33.

Ilisz, I., Dombi, A., Mogyorósi, K., Farkas, A., Dékány, I., 2002. Removal of 2-chlorophenol from water by adsorption combined with TiO_2 photocatalysis. Appl. Catal. B: Environ. 39, 247–256.

Iwasaki, M., Hara, M., Kawada, H., Tada, H., Ito, S., 2000. Cobalt Ion-Doped TiO_2 Photocatalyst Response to Visible Light. J. Colloid Interface Sci. 224, 202–204.

Jaffrezic-Renault, N., Pichat, P., Foissy, A., Mercier, R., 1986. Study of the effect of deposited platinum particles on the surface charge of titania aqueous suspensions by potentiometry, electrophoresis, and labeled-ion adsorption. J. Phys. Chem. 90, 2733–2738.

Jung, O.-J., 2001. Synergistic effect on the photocatalytic degradation of 2-chlorophenol using TiO_2 thin films doped with some transition metals in water. Bull. Korean Chem. Soc. 22, 1183–1191.

Jung, O.J., Kim, S.H., Cheong, K.H., Li, W., Shah, S.I., 2003. Metallorganic chemical vapor deposition and characterization of TiO_2 nanoparticles. Bull. Korean Chem. Soc. 24, 49–54.

Kovalenko, A.S., Kuchmii, S. Ya., Makovskaya, T.F., Korzhak, A.V., Tsyrina, V.V., Yatskiv, V.I., Ilin, V.G., 2003. Effect of Metal Inclusions on the Porous Structure and Photocatalytic Activity of Titanium Dioxide. Theor. Exp. Chem. 39 (2), 119–125.

Krijgsheld, K.R., van der Gen, A., 1986. Assessment of the impact of the emission of certain organochlorine compounds on the aquatic environment: part I: monochlorophenols and 2,4-dichlorophenol. Chemosphere 15, 825–860.

Ku, Y., Leu, R.-M., Lee, K.-C., 1996. Decomposition of 2-chlorophenol in aqueous solution by UV irradiation with the presence of titanium dioxide. Wat. Res. 30, 2569–2578.

Leofanti, G., Padovan, M., Tozzola, G., Venturelli, B., 1998. Surface area and pore texture of catalysts. Catal. Today 41, 207–219.

Li, G.H., Chen, L., Graham, M.E., Gray, K.A., 2007. A comparison of mixed phase titania photocatalysts prepared by physical and chemical methods: The importance of the solid–solid interface. J. Mol. Catal. A: Chem. 275, 30–35.

Liu, G., Wang, X., Chen, Z., Chen, H.-M., Qing (Max) Lu, G., 2009. The role of crystal phase in determining photocatalytic activity of nitrogen doped TiO_2. J. Colloid Interface Sci. 329, 331–338.

Madhu Kumar, P., Badrinarayanan, S., Sastry, M., 2000. Nanocrystalline TiO_2 studied by optical, FTIR and X-ray photoelectron spectroscopy: correlation to presence of surface states. Thin Solid Films 358, 122–130.

Nahar, M.S., Hasegawa, K., Kagaya, S., 2006. Photocatalytic degradation of phenol by visible light-responsive iron-doped TiO_2 and spontaneous sedimentation of the TiO_2 particles. Chemosphere 65, 1976–1982.

Nahar, M.S., Zhang, J., Hasegawa, K., Kagaya, S., Kuroda, S., 2009. Phase transformation of anatase–rutile crystals in doped and undoped TiO_2 particles obtained by the oxidation of polycrystalline sulfide. Mater. Sci. Semiconductor Process. 12, 168–174.

Ozkan, S., Kumthekar, M.W., Karakas, G., 1998. Characterization and temperature-programmed studies over Pd/TiO_2 catalysts for NO reduction with methane. Catal. Today 40, 3–14.

Piera, E., Tejedor-Tejedor, M.I., Zorn, M.E., Anderson, M.A., 2003. Relationship concerning the nature and concentration of Fe(III) species on the surface of TiO_2 particles and photocatalytic activity of the catalyst. Appl. Catal. B 46, 671–685.

Puma, G.L., Yue, P.L., 2002. Effect of radiation wavelength on the rate of photocatalytic oxidation of organic pollutants. Ind. Eng. Chem. Res. 41, 5594–5600.

Ragaini, V., Selli, E., Bianchi, C.L., Pirola, C., 2001. Sono-photocatalytic degradation of 2-chlorophenol in water: kinetic and energetic comparison with other techniques. Ultrason. Sonochem. 8, 251–258.

Rideh, L., Wehrer, A., Ronze, D., Zoulalian, A., 1997. Photocatalytic degradation of 2-chlorophenol in TiO_2 aqueous suspension: modeling of reaction rate. Ind. Eng. Chem. Res. 36, 4712–4718.

Roques, H., 1996. Chemical Water Treatment. VCH Verlag, Wienheim, Germany.

Senthilnanthan, M., Ho, D.P., Vigneswaran, S., Ngo, H.H., Shon, H.K., 2010. Visible light responsive ruthenium-doped titanium dioxide for the removal of metsulfuron-methyl herbcide in aqueous phase. Sep. Purif. Technol. 75, 415–419.

Shen, M., Wu, Z.Y., Huang, H., Du, Y., Zou, Z., Yang, P., 2006. Carbon-doped anatase TiO_2 obtained from TiC for photocatalysis under visible light irradiation. Mater. Lett. 60, 693–697.

Shen, X., Garces, L.J., Ding, Y., Laubernds, K., Zerger, R.P., Aindow, M., Neth, E.J., Suib, S.L., 2008. Behavior of H_2 chemisorption on Ru/TiO_2 surface and its application in evaluation of Ru particle sizes compared with TEM and XRD analyses. Appl. Catal. A: Gen. 335, 187–195.

Song, G.B., Liang, J.K., Liu, F.S., Peng, T.J., Rao, G.H., 2005. Preparation and phase transformation of anatase–rutile crystals in metal doped TiO_2/muscovite nanocomposites. Thin Solid Films 491, 110–116.

Sun, B., Smirniotis, P.G., Boolchand, P., 2005. Visible light photocatalysis with platinized rutile TiO_2 for aqueous organic oxidation. Langmuir 21, 11397–11403.

Tomul, F., Balci, S., 2009. Characterization of Al, Cr-pillared clays and CO oxidation. Appl. Clay Sci. 43, 13–20.

Tsai, S.-J., Cheng, S., 1997. Effect of TiO_2 crystalline structure in photocatalytic degradation of phenolic contaminants. Catal. Today 33, 227–237.

Tseng, I.-H., Chang, W.C., Wu, J.C.S., 2002. Photoreduction of CO_2 using sol–gel derived titania and titania-supported copper catalysts. Appl. Catal. B: Environ. 37, 37–48.

Tseng, I.-H., Wu, J.C.S., Chou, H.-Y., 2004. Effects of sol–gel procedures on the photocatalysis of Cu/TiO_2 in CO_2 photoreduction. J. Catal. 221, 432–440.

Venkatachalam, N., Palanichamy, M., Arabindoo, B., Murugesan, V., 2007. Enhanced photocatalytic degradation of 4-chlorophenol by Zr^{4+} doped nano TiO_2. J. Mol. Catal. A: Chem. 266, 158–165.